**Technical Annals**

Vol 1, No 5 (2024)

Technical Annals

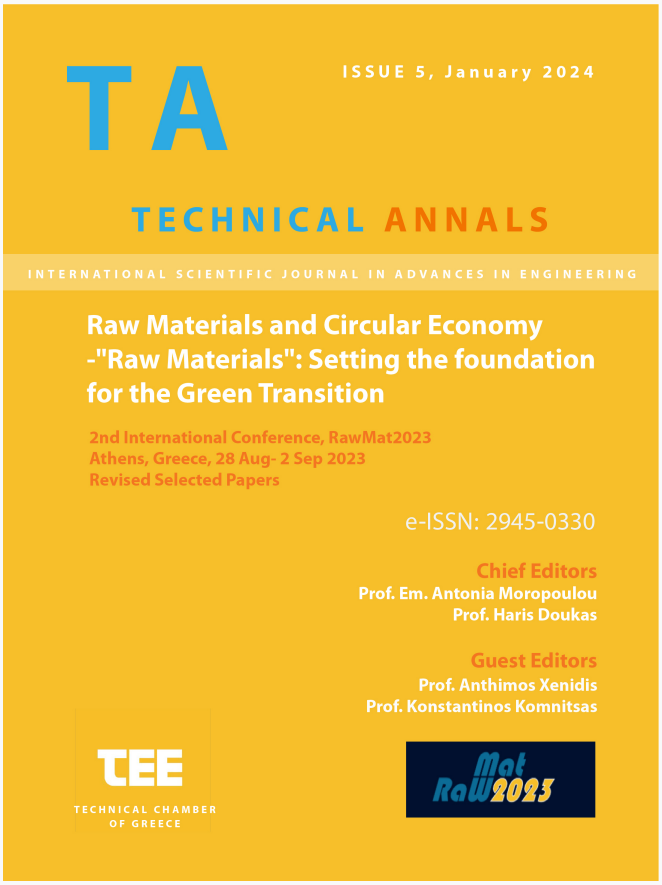


# Corrosion and Tensile Behavior of 304L Rebars under the Influence of a Concrete Additive and Migrating Corrosion Inhibitors

*Sofia Tsouli, Spiridon Kleftakis, Angeliki G. Lekatou*

doi: 10.12681/ta.39102



**To cite this article:**

Tsouli, S., Kleftakis, S., & Lekatou, A. G. (2024). Corrosion and Tensile Behavior of 304L Rebars under the Influence of a Concrete Additive and Migrating Corrosion Inhibitors. *Technical Annals*, *1*(5). https://doi.org/10.12681/ta.39102

# Corrosion and Tensile Behavior of 304L Rebars under the Influence of a Concrete Additive and Migrating Corrosion Inhibitors

S. Tsouli[1] [0000-0002-5703-9403], S. Kleftakis[1], A.G. Lekatou[1,*] [/0000-0001-7951-4431]

[1]Laboratory of Applied Metallurgy, Department of Materials Science and Engineering, School of Engineering, University of Ioannina, 45110 Ioannina, Greece
*alekatou@uoi.gr

**Abstract.** This study examines the effect of a Ca-rich fly ash additive, a liquid migrating corrosion inhibitor (Inhibitor B), and a vapor phase inhibitor (Inhibitor C), individually and in combination, on the corrosion performance of 304L stainless steel rebars embedded in concrete cubes. This was assessed through open circuit potential (OCP) measurements over 1 m in an acid rain (AR) simulating electrolyte, salt spray testing for 4 m and tensile testing of 304L rebars following the corrosion tests. For 304L rebars embedded in concrete cubes containing fly ash (FA), Inhibitor B, Inhibitor C, and combinations of FA with Inhibitor B, immersed in AR for 1 m during OCP testing, there was more than a 90% probability that corrosion did not occur. Both Inhibitors B and C improved the corrosion resistance of the rebars in AR in the absence of FA, but when combined with FA, their inhibiting effects were neutralized. The 20 wt.% FA content improved the corrosion behavior of 304L rebars compared to 0 wt.% FA. After 1 m of OCP testing in AR, % elongation increased in all cases except without inhibitors. After 4 m of salt spraying, a slight decrease in strength was observed for the 304L reinforcement, both in the absence and presence of any inhibitors, though within standard deviation.

**Keywords:** 304L stainless steel rebars, Migrating Corrosion Inhibitors, Fly Ash, Salt Spray Test, Open Circuit Potential test.

## 1 Introduction

Steel reinforcement corrosion is the primary cause of reinforced concrete structure degradation, as it weakens the steel/concrete bond strength [1,2] and the concrete durability [3,4]. Various methods have been employed to mitigate this issue, including (i) alternative reinforcement materials and slab designs, (ii) barrier techniques, (iii) corrosion inhibitors and (iv) electrochemical procedures [5].

Among alternative reinforcement materials, stainless steel, molten zinc and epoxy-sprayed bars and stainless steel claddings offer the highest resistance to corrosion. However, solid stainless steel rebars provide superior structural properties [6]. Though more expensive than carbon steel, the long-term savings from reduced maintenance and

replacement costs often justify the initial investment on stainless steel rebars [1]. As a result, stainless steel rebars are increasingly used in new concrete constructions and renovations, especially in critical areas exposed to corrosive conditions [1], as well as in restoration works of ancient monuments and historical buildings like the ancient theater of Dodona in Epirus, Greece, where AISI 316L stainless steel is employed [7].

Barrier methods include partial replacement of cement with mineral additives, such as fly ash, silica fume, blast furnace slag, calcite laterites and microsilica, use of concrete overlays, waterproof membranes, concrete sealers and deep polymer impregnation [5]. The partial replacement of cement with mineral additives, such as fly ash (FA), has been a reliable, economic and environmentally friendly method to limit corrosion of reinforced concrete in aggressive environments including acidic [8, 9]. The addition of fly ash (FA) to concrete can enhance corrosion resistance by forming calcium silicate hydrate (C-S-H) through the pozzolanic reaction, which consumes the less stable calcium hydroxide (C-H) and fills concrete's capillary voids [8, 9]. FA also refines the concrete's pore structure by reducing pore volume, distribution, and critical pore size [9]. Furthermore, FA increases resistance to chloride, sulfate, sulfuric acid, and nitric acid attacks by forming pozzolanic products like Friedel's salt and ettringite, which decrease concrete permeability [8, 10].

Corrosion inhibitors can be a good alternative to other protection methods due to their low cost and ease of application [11]. They can be classified according to the electrochemical mechanisms of protection to: (a) anodic, (b) cathodic and (c) mixed, depending on whether they affect (a) the anodic reaction (steel dissolution), (b) the cathodic reaction on the steel surface or (c) both reactions by acting on both anodic and cathodic sites. They can also be classified according to the application methods to (a) admixed corrosion inhibitors (mixed into fresh concrete for new structures) and (b) migrating corrosion inhibitors - MCIs (applied onto the surface of hardened concrete, often to repair reinforced concrete) [11-13].

MCI molecules can migrate through concrete pores via liquid capillary action and gaseous phase diffusion onto the surface of the steel reinforcement, where they chemically interact with it and form a stable layer that shields both the anodic and cathodic sites of the rebars. [13, 14]. Active groups of MCIs can also adsorb chloride ions preventing them from directly accessing the steel [15]. Additionally, MCIs block surface pores in concrete, primarily at the surface rather than in the bulk, enhancing anti-corrosion effects without affecting the concrete's physical and mechanical properties [13, 16, 17]. In cases of pitting, inhibitors can function by [11]: a) forming a protective film before chloride ingress, b) stabilizing the pH in and around the pit, c) competing with aggressive ions for surface adsorption, and d) competing with aggressive ions for migration into the pit.

Amines, alkanolamines (AMA), and their salts with organic and inorganic acids are common inhibitors for protecting concrete steel reinforcement [11]. While MCIs are mostly considered to exert a mixed electrochemical action because they form a layer on both anodic and cathodic sites [11, 14], some studies suggest a mainly cathodic [18] or mainly anodic action [19]. The AMA-based inhibitors consist of a volatile aminoal-

cohol and an acid that forms a salt with the aminoalcohol [11]. Typical AMA compounds include diethanolamine, dimethylpropanolamine, monoethanolamine, and dimethylethanolamine [17].

A main issue with MCIs is the difficulty of the surface applied volatile liquid to migrate through the concrete to the steel surface. For this reason, capsule-contained volatile (or vapor phase) corrosion inhibitors (VCIs or VPIs) have been developed, which can be inserted into drilled holes near the steel [20]. These capsules release volatile phases of varying vapor pressures ensuring a controlled release over time. These volatile phases diffuse to the metal surface, condense, physically adsorb onto it, and form a thin film of crystals. In the presence of even traces of moisture, the crystals dissolve, polarize and are attracted to the metal's anode and cathode, forming a protective layer that thickens over time by condensation of vapors [21]. Effective VCIs are typically salts of weak volatile acids and bases, like amine salts, ensuring both protection and volatility [22, 23]. The pH of the moisture film should be balanced, neither too acidic nor too alkaline [22].

Previous studies by the authors have demonstrated that high-calcium fly ash (FA) can replace both $Ca(OH)_2$ and Portland cement up to 20 wt.% enhancing the corrosion resistance of 316L and 304L stainless steel rebars in acid rain simulating solutions, seawater simulating solution and simulated saline environments attacked by acid rain [7, 24-29]. However, increasing FA to 25 wt.% reverses this trend owing to the formation of agglomerates that have reduced tendency for pozzolanic or cementitious reactions and also form differential aeration cells on the steel beneath them. The feasibility of using 304L stainless steel instead of 316L in critical applications, like historic monument restoration, was demonstrated. This substitution was achievable by incorporating low FA concentrations (10 or 15 wt.%) in both slightly acidic and strongly alkaline environment [26, 27]. Replacing cement with up to 25 wt.% FA in concrete had not any significant effect on the tensile properties of 316L and 304L rebars before and after 4 m of salt spraying [26, 28]. Additionally, FA, alone or combined with a liquid corrosion inhibitor, reduced porosity after salt spraying, with the most significant reduction observed at 15% and 25% FA content [30].

The current investigation is part of a broader initiative aimed at holistically exploring the potential of incorporating high-Ca fly ash in concrete members of critical applications. Studies assessing the performance of stainless steels embedded in concrete mixes containing high-calcium fly ash in acid rain environments are scarce, primarily due to concerns regarding the utilization of high-calcium fly ash. The latter contains elevated levels of free CaO and S, which are considered to negatively impact volume stability and concrete durability [31]. Additionally, high Ca-FAs contain significant quantities of $Al_2O_3$ in their glassy phase, which may react with C-H produced during cement hydration to form calcium aluminate hydrate (C-A-H); interaction with sulfate-rich environments, may lead to the formation of heavily hydrated ettringite causing expansion-related cracking [10]. On the other hand, certain mineralogical characteristics of high-calcium fly ash, such as engagement of $Al_2O_3$ in inert phases, supersulfation of concrete, selective nucleation of the corrosion resistant C-S-H on the surface of the $CaCO_3$ contained in the fly ash, can counteract the adverse effects mentioned earlier; further details can be sought in [27].

Within the above framework, the present effort focuses on the effect of FA, combined with a liquid inhibitor and a gas phase inhibitor, on: (a) the corrosion performance of 304L rebars embedded in concrete cubes during open circuit potential (OCP) measurements over a period of 1 m in an electrolyte simulating acid rain, and (b) the mechanical properties of 304L rebars embedded in concrete cubes subjected to salt fog testing for 4 m. The main motivation for this effort stems from the fact that several investigations have suggested that the amine-based inhibitors have a limited effect on corrosion inhibition [15, 32]. Also, a combination of two or more types of inhibitors could offer an effective strategy for enhancing corrosion protection [14, 15].

## 2 Experimental

304L stainless steel corrugated rebars having nominal composition in wt.%: Fe, 0.03% C, 18.20% Cr, 8.51% Ni, 0.75% Si, 2.00% Mn, 0.045% P, 0.03% S, diameter of 6 mm and length of 12 cm were embedded in concrete cubes. The concrete cubes ($7\times7\times7$ $cm^3$) contained Portland cement (CEM II/A-M 42.5R), CEN Standard silica sand and water (cement/sand/water: 450/225/1350 (g), according to BS EN 196-1). XRD analysis of the concrete mixture after hydration for 24 h detected the following hydration products along with calcite ($CaCO_3$): various C-S-H ($CaO\text{-}SiO_2\text{-}H_2O$) minerals that constitute the main hydration product of cement, other hydration minerals, like $CaO_2\cdot8H_2O$, C-H, C-A-Š-H ($CaO\text{-}Al_2O_3\text{-}SO_2\text{-}H_2O$) and C-A-H, and sulfoaluminates Aft (ettringite) and Afm (monosulfoaluminate) [27].

Pulverized class-C fly ash (FA) from the Hellenic Public Power Corporation lignite mines in Western Macedonia, Greece, was also added in the concrete mixture, FA replacing 20 wt.% of cement. The FA was mainly composed by CaO, $SiO_2$, $Al_2O_3$, $SO_3$, $Fe_2O_3$, and MgO [7]. A comprehensive mineralogical analysis of the FA is provided in [27]. In summary, the FA primarily consisted of calcite ($CaCO_3$), anhydrite ($CaSO_4$), quartz ($SiO_2$), lime (CaO), and hematite ($Fe_2O_3$). Minerals present in minor quantities included brownmillerite ($Ca_2(Al,Fe)_2O_5$), periclase (MgO), merwinite ($Ca_3Mg(SiO_4)_2$), portlandite ($Ca(OH)_2$), K-Al-silicates like K-feldspars and illite, and traces of plagioclase. Amorphous phases including glass and residual clay minerals from lignite, were also identified. Among the aforementioned minerals, anhydrite, lime, brownmillerite, periclase, and portlandite are reactive minerals, while quartz, hematite, and K-Al silicates are inert [33]. Consequently, the high content of reactive minerals (particularly anhydrite and lime) along with glassy phases in the fly ash imparts it with hydraulic and pozzolanic properties, making this fly ash a potentially effective binding agent [34].

Inhibitor B, a liquid MCI inhibitor with a mixed electrochemical action, based on alkanolamine, was applied by brush on the concrete surface. Besides its corrosion inhibition by molecule migration, as described in the Introduction, it is claimed to restore the alkalinity of the concrete and maintain it stable [35]. Inhibitor C, a third generation VCI inhibitor, released in three stages, was inserted in concrete cubes, as a 10 ml capsule. Inhibitor C is made up of a complex blend of three vapour phase corrosion inhibitors of fast (24 h), medium (48 h) and long (12-48 m) term protection, resulting in the building of a protective passive film around the reinforcement. Inhibitor C works as a

migrating corrosion inhibitor of anodic and cathodic action by building a vapour density within an enclosed space. [36].

The open circuit potential (OCP test) of reinforced concrete cubes immersed in an acid rain simulating electrolyte ((g/L $H_2O$): $H_2SO_4$: 0.032, $HNO_3$: 0.015, $(NH_4)_2SO_4$: 0.046, $Na_2SO_4$: 0.032, $NaNO_3$: 0.021 and NaCl: 0.084, pH = 3.1 [37]) was recorded every 10 min for 1 m. The stainless steel /concrete junction of the free surface was coated by an epoxy glue. The naked part of the rebar was connected with the ACM Gill AC potentiostat using a three electrode cell (reference electrode: Ag/AgCl/3.5 M KCl, counter electrode: Pt-gauge). The pH value of the electrolyte was regularly measured.

The reinforced concrete cubes also underwent salt spraying for 4 m in a Vötch chamber using a fog of 5 wt.% NaCl at 35 ºC according to ASTM B117-97.

Prior to and after salt spray and OCP tests, the rebars were carefully removed from the concrete cubes and were subjected to tensile testing at the Galdabini uniaxial testing machine (100 kN, cross-head speed: 1.30 mm/min, ASTM E8/E8M-09).

Polished cross sections of 304L after the OCP and salt spraying tests were examined by Scanning Electron Microscopy and Energy Dispersion X-ray Spectroscopy (SEM/EDX) at the JeoL JSM 6510 LV system, equipped with an X-act (Oxford Instr.) EDX analyzer.

# 3 Results and discussion

## 3.1 OCP test

Figs. 1a-e illustrate the variation of the OCP values of 304L rebars embedded in concrete cubes containing FA (0 wt.% & 20 wt.%) and/or Inhibitors B and C. It should be noted that the OCP test is an electrochemical technique that does not provide any information about the corrosion kinetics, but identifies the existence of corrosion or passivation [38]. In all cases, the OCP values are more positive than -160 mV (Ag/AgCl), indicating a greater than 90% probability that the rebars are in a non-corroding state [38, 39]. The only exception is the case of "304L - 0 wt.% FA + Inhibitor C" during the first three to four days of immersion (Fig. 1c,e), after which the OCP ennobles, following a continuously increasing trend. As reported in the Experimental section, this ennoblement coincides with the vaporization of the medium term component of Inhibitor C, which strengthens the bonding of the surface film with the steel.

The intensive fluctuations in the OCP values in Fig. 1, provide evidence of the alternating formation and dissolution of surface products on steel surface sites that are most susceptible to pitting, like strain-hardened martensitic ribs and sulfide inclusions. Nevertheless, pitting is metastable and has led to repassivation, since OCP > -160 mV (Ag/AgCl). Pitting in 304L steel is usually associated with MnS inclusions [40].

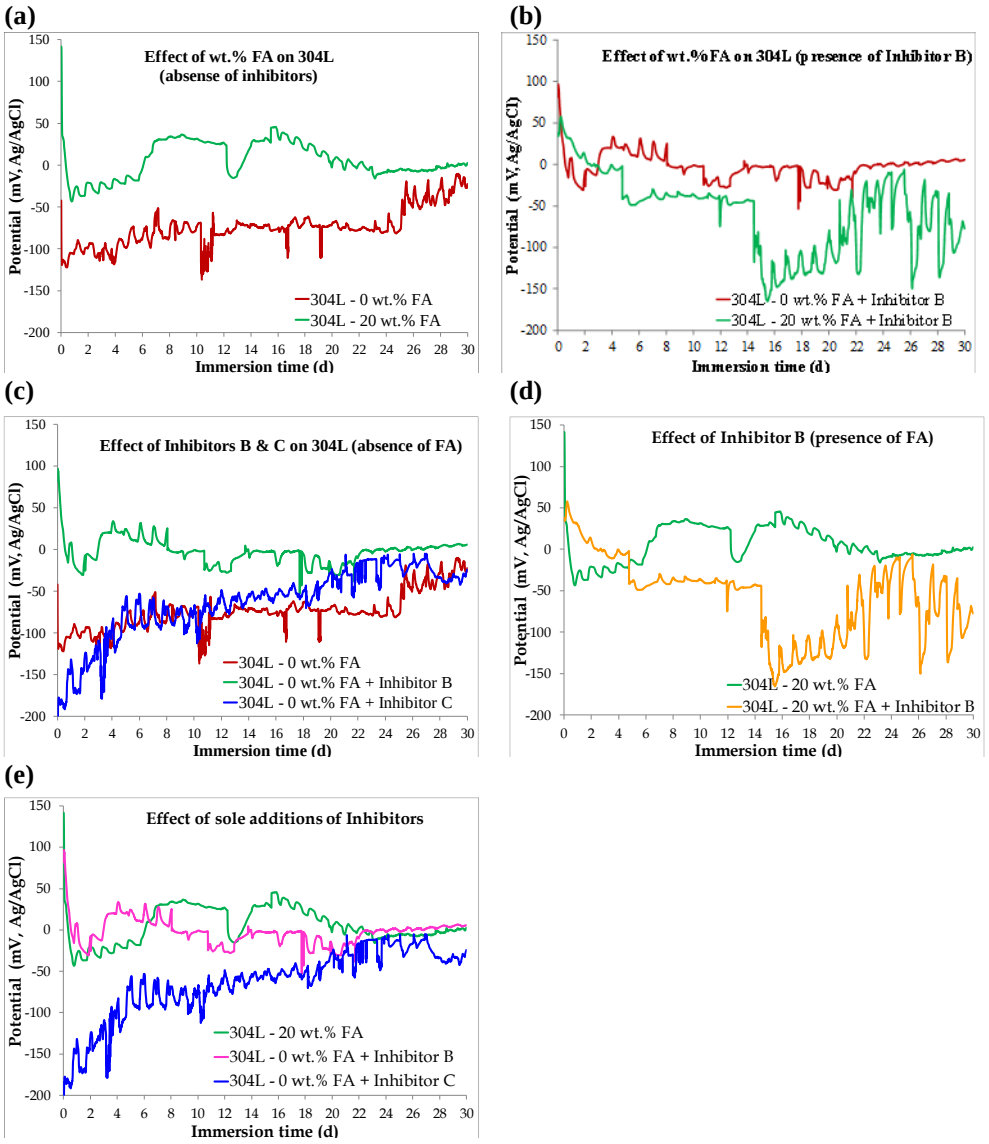


**Fig. 1.** Open circuit potential measurements of concrete embedded 304L rebars immersed in a simulating acid rain solution (pH = 3.1)

In Fig. 1b, the notably higher OCP values and reduced OCP fluctuations indicate that the 20 wt.% FA content has a beneficial effect on the corrosion behavior of 304L rebars compared to 0 wt.% FA. This observation aligns with previous studies by the authors, which elaborate on the beneficial role of FA [7, 24-30]. The beneficial role of FA under AR attack can be attributed to its high content of reactive phases with hydraulic and pozzolanic properties. Additionally, a significant portion of $Al_2O_3$ in FA

has been shown to be bound in inert K-Al silicate minerals, which limits the availability of alumina to form ettringite [27]. Ettringite ($C_3A(CS)_3H_{32}$) is a compound that can expand nearly sevenfold in volume leading to internal stresses and subsequent cracking of concrete [26].

Fig. 1c shows that both Inhibitors B and C improved the corrosion behavior of 304L concrete reinforcement in the absence of FA, with Inhibitor B demonstrating the best resistance to corrosion for up to 20 d of immersion. After this period, Inhibitors B and C led to similar corrosion performances. It should be emphasized that the long term component of Inhibitor C had not been released by the end of the test; hence, its full potential had not been realized.

Conversely, the combination of FA with Inhibitor B for 304L rebars shows worse corrosion performance compared to the use of Inhibitor B alone (Fig. 1b) or FA alone (Fig. 1d) in terms of lower OCP values and more intensive OCP fluctuations. Hence, it is drawn that the combination of Inhibitor B with FA has negated the individual inhibiting effects of both FA and Inhbitor B, as sole additions. This conclusion is compatible with previous research by the authors, which showed that the combination of FA with Inhibitor B slightly increases the porosity of concrete compared to the sole addition of FA, although within statistical error [30]. A similar conclusion was drawn in that study for the combination of FA with Inhibitor C. Fig. 1e shows that the OCP values in the presence of inhibitors B, C and FA, converge after 22 d of immersion. It should again be noted that the long term component of Inhibitor C had not been released by the end of the OCP test.

### 3.2 Tensile testing after salt spray and OCP tests

Fig. 2 shows the macroscopic state of concrete cubes reinforced with 304L rebars after having been subjected to a salt spray test for 4 m. The concrete cubes in Fig. 1a,b contain 20 wt.% FA and are coated by Inhibitor B, whereas in Fig. 1c,d contain 20 wt.% FA and Inhibitor C. Both cases manifest excellent surface states without any visible signs of corrosion. Fig. 3 presents the stress-strain curves of 304L rebars extracted from concrete cubes, which either contained 20 wt.% FA (Fig. 3a, b) or did not (Fig. 3c, d), and were either coated with Inhibitor B (Fig. 3b, d) or not (Fig. 3a, c), before and after 4 m of salt spray testing. The only notable difference in Fig. 3 is the decreased strain in the specimens after salt spraying. Fig. 3d shows that the decreasing trend in the strain is consistent over the time span from 0 to 4 m. Similarly, Fig. 4 presents the stress-strain curves of 304L rebars extracted from concrete cubes, which either contained 20 wt.% FA (Fig. 4a, b) or did not (Fig. 4c, d), and were either coated with Inhibitor B (Fig. 4b, d) or not (Fig. 4a, c), before and after 1 m of OCP testing. The only noticeable difference in Fig. 4 is the increased strain of the specimens removed from the cubes containing 20 wt.% FA and/or Inhibitor B, after OCP testing, in contrast to the slightly decreased strain of the specimens removed from the concrete cube free of any inhibitors (the latter is observed in Fig. 4c). This increase is in contrast with the decreased strain after salt spraying. Table 1 compares the effect of FA, Inhibitor B and their combination on the tensile property values of 304L rebars removed from concrete cubes after salt spray testing (4 m) and OCP testing (1 m). It can be seen that after salt spray test and

after OCP test, the presence of 20 wt.% FA and/or Inhibitor B does not have any statistically significant effect on the tensile properties of 304L rebars. Table 2 presents the effect of time on the tensile properties of 304L rebars removed from concrete cubes prior to and after salt spray testing (4 m) and OCP testing (1 m).

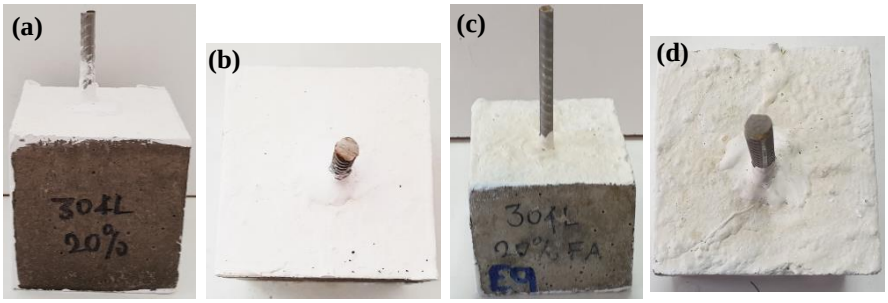


**Fig. 2.** Concrete cubes reinforced by 304L rebars after salt spraying for 4 m: (a), (b): 20 wt.% fly ash + Inhibitor B; (c), (d): 20 wt.% fly ash + Inhibitor C

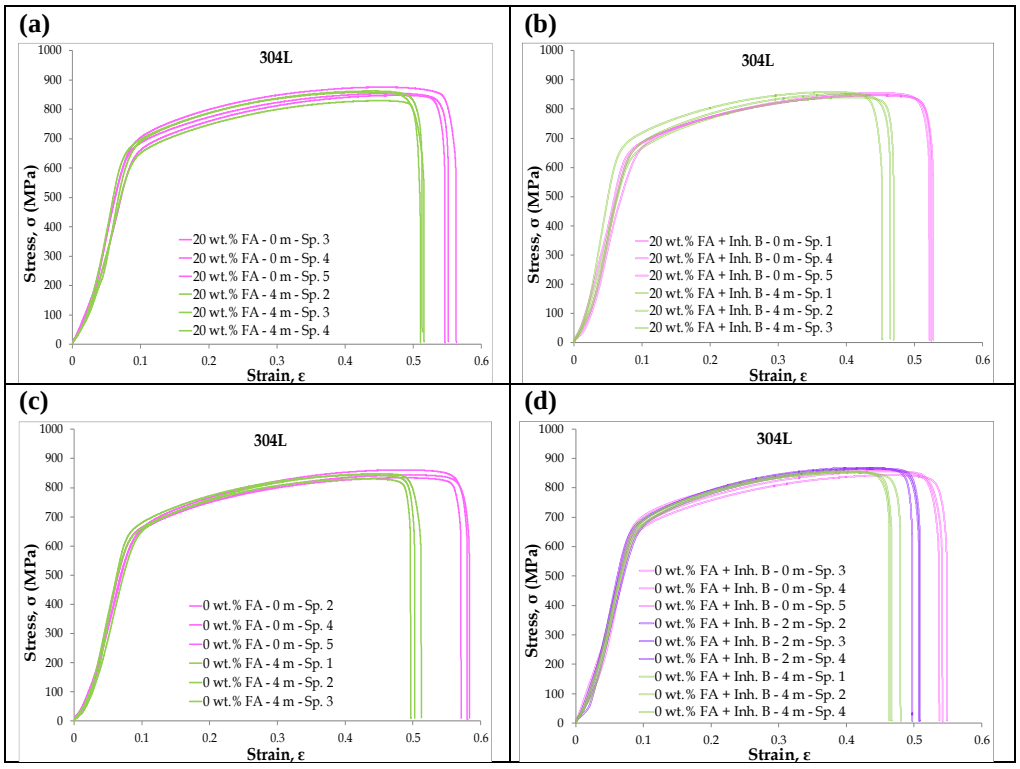


**Fig. 3.** Stress-strain curves of 304L corrugated bars reinforcing concrete that contained: (a) 20 wt.% fly ash, (b) 20 wt.% fly ash + Inhibitor B, (c) 0 wt.% fly ash, (d) 0 wt.% fly ash + Inhibitor B, before (0 m) and after salt spraying for 4 m (4 m)

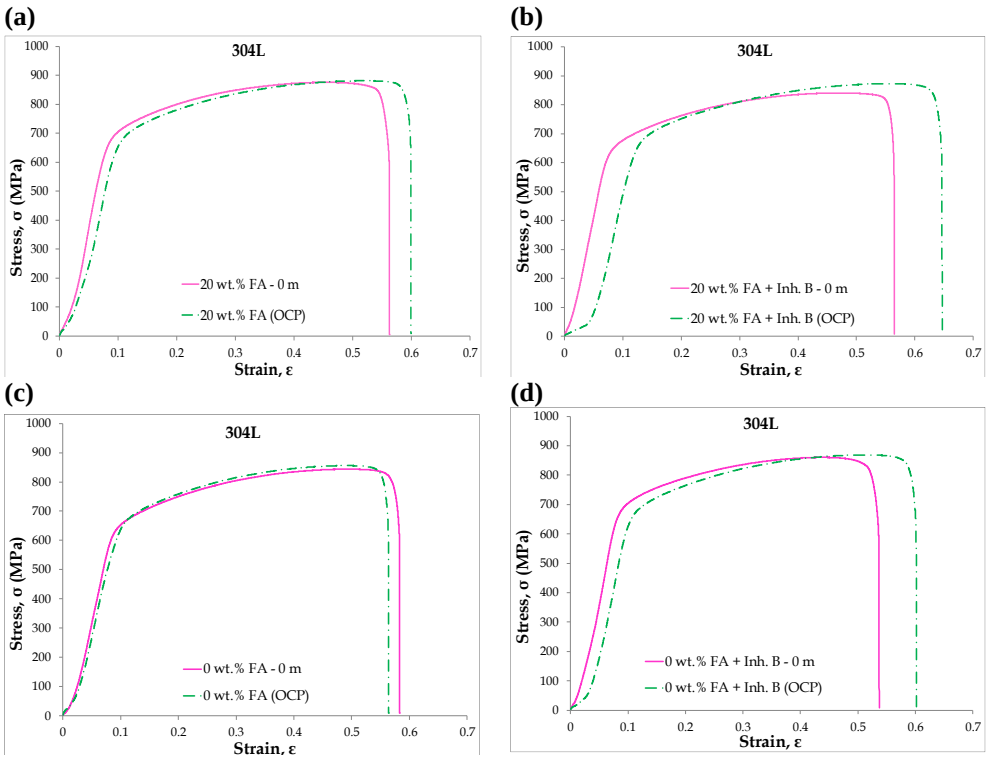


**Fig. 4.** Stress-strain curves of 304L corrugated bars reinforcing concrete that contained: (a) 20 wt.% fly ash, (b) 20 wt.% fly ash + Inhibitor B, (c) 0 wt.% fly ash, (d) 0 wt.% fly ash + Inhibitor B, before (0 m) and after OCP testing for 1 m (OCP)

**Table 1.** Effect of fly ash, inhibitor B and their combination on the tensile properties of 304L rebars after salt spray testing (4 m) and OCP testing (1 m)

| Inhibitor | Test | Duration, m | 0.2% yield strength, MPa | Tensile strength, MPa | Fracture strength, MPa | % el |
|---|---|---|---|---|---|---|
| 0FA, 0B | Salt spray | 4 | 537±18 | 702±17 | 718±13 | 38±1 |
| 20FA | Salt spray | 4 | 571±56 | 738±71 | 680±47 | 40±4 |
| B | Salt spray | 4 | 509±61 | 662±61 | 631±62 | 34±1 |
| 20FA+B | Salt spray | 4 | 546±43 | 706±47 | 666±47 | 34±1 |
| 0FA, 0B | OCP | 1 | 540±36 | 699±40 | 699±60 | 41±2 |
| 20FA | OCP | 1 | 551±38 | 713±55 | 713±54 | 44±2 |
| B | OCP | 1 | 552±47 | 714±51 | 714±37 | 45±2 |

**Table 2.** Effect of time on the tensile properties of 304L rebars prior to and after salt spray testing (4 m) and OCP testing (1 m).

| Inhibitor | Test | Duration, m | 0.2% yield strength, MPa | Tensile strength, MPa | Fracture strength, MPa | % el |
|---|---|---|---|---|---|---|
| 0FA, 0B | Salt spray | 0 | 597±15 | 780±28 | 751±40 | 44±1 |
| 0FA, 0B | Salt spray | 4 | 573±11 | 739±14 | 718±13 | 37±1 |
| 20FA | Salt spray | 0 | 586±15 | 754±16 | 707±9 | 43±1 |
| 20FA | Salt spray | 4 | 571±56 | 738±71 | 680±47 | 40±4 |
| B | Salt spray | 0 | 583±44 | 751±51 | 717±40 | 43±1 |
| B | Salt spray | 4 | 509±61 | 662±61 | 631±62 | 34±1 |
| 20FA+B | Salt spray | 0 | 554±36 | 709±32 | 678±33 | 42±2 |
| 20FA+B | Salt spray | 4 | 546±43 | 706±47 | 666±47 | 36±1 |
| 0FA, 0B | OCP | 0 | 572±25 | 747±36 | 712±42 | 43±1 |
| 0FA, 0B | OCP | 1 | 540±36 | 699±40 | 699±60 | 41±2 |
| 20FA | OCP | 0 | 543±59 | 680±50 | 643±45 | 40±2 |
| 20FA | OCP | 1 | 551±38 | 713±55 | 713±54 | 44±2 |
| B | OCP | 0 | 543±50 | 680±50 | 643±45 | 40±2 |
| B | OCP | 1 | 552±47 | 714±51 | 714±37 | 45±2 |
| 20FA+B | OCP | 0 | 554±36 | 709±32 | 678±33 | 42±2 |

Table 2 shows that after 4 m of salt spraying, 304L reinforcement presented a slight decrease in the strength values, though within standard deviation. The drops in the strength values were larger in the case of single use of Inhibitor B than the drops in the cases of 20FA and 20FA+Inhibitor B. Small decreases % elongation (with or without inhibitors) were also observed. The drops in the % elongation were statistically significant in all cases but 20 wt.% FA. The above observations are in compatibility with Lee et al. [40] and Apostolopoulos et al. [41], who observed that the corrosion effect on the elongation of concrete steel rebar is more intensive compared to its yield strength and tensile strength. The decrease in elongation has been associated with embrittleness due to pitting, as microcracking initiates at pits [40].

The largest drop in %el after salt spraying, occurred when FA was absent from the concrete (cases 0FA-0B, 0FA-B). The smallest drop in %el occurred in the cases of 20FA-0B (especially) and 20FA-B. This observation is consistent with the decrease in the concrete porosity after four months of salt spraying, realized by the addition of FA in the concrete (either alone or combined with inhibitor B) [30]. Previous authors' work has demonstrated that high Ca-FA as a concrete additive boosts the pozzolanic reactions in the concrete through the formation of Ca-Al-Fe-silicate hydroxides that are more stable than $Ca(OH)_2$ [27]. As the curing time increases with salt spraying, more hydration products are formed that can protect by simply reducing the concrete porosity (e.g. just forming $Ca(OH)_2$ [42]) or by both reducing the concrete porosity and forming stable compounds.

Despite the small drop in %el. after salt spraying, Fig. 5 does not reveal any significant differences in the fracture modes of 304L rebars before and after salt spraying for 4 m. The rebars have been removed from concrete cubes containing 25 wt.% FA and

being coated by inhibitor B. The low magnification images (for a more objective observation) reveal that the ductile mode of fracture has been retained after 4 m of salt spraying. The fracture surfaces are characterized by numerous dimples, a result of the stretching and thinning of the material during deformation [43]. Elongated dimples have been formed by microvoid coalescence.

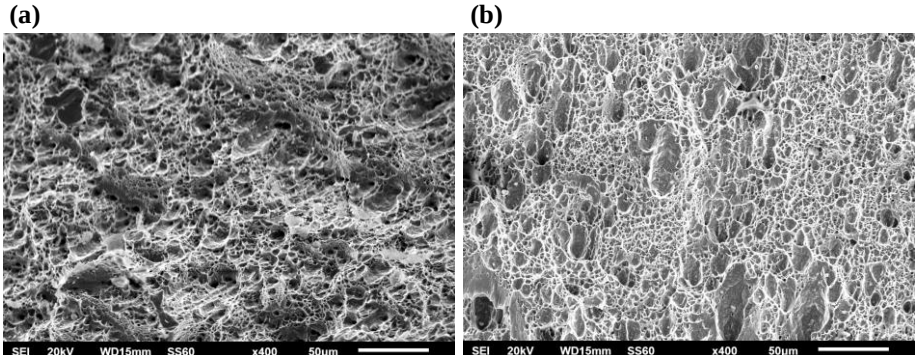


**Fig. 5.** Fracture surfaces of 304L concrete rebars after tensile testing (a) before and (b) after 4 m of salt spraying. The rebars have been removed from concrete cubes containing 25 wt.% fly ash and coated by inhibitor B.

Table 2 shows that after 1 m in OC state in the AR simulating electrolyte, the strength values of 304L rebars in the absence of inhibitors and FA, showed small decreases, though within standard deviation. The tensile properties of 304L, in the sole presence of 20 wt.% FA concrete additive or Inhibitor B, showed a statistical but consistent increase. In the case of combined "20 wt.% FA + Inhibitor B", the strength values remained practically unchanged. All the same, in all cases, % el. has increased.

In the case of FA addition, previous authors' work has shown that high Ca-FA as a concrete additive has led to formation of new phases, such as aluminum sulfate/sulfite hydrates that supersulfate the concrete, inhibiting its reaction with the sulfate ions of acid rain to form expansive compounds that may lead to concrete cracking [27].

In the case of Inhibitor B, one or more of the mechanisms reported in the Introduction can be considered responsible for this slight improvement in the tensile properties. For instance, Fig. 6 shows that the presence of Inhibitors B and C, induce small increases in the pH of the electrolyte compared to the sole addition of 20 wt.% FA. Although this result is not conclusive, it indicates that Inhibitors B and C can stabilize the pH within the pit's immediate environment. Other potential beneficial mechanisms of the inhibitors will be discussed in conjunction with the SEM/EDX examination in the next section.

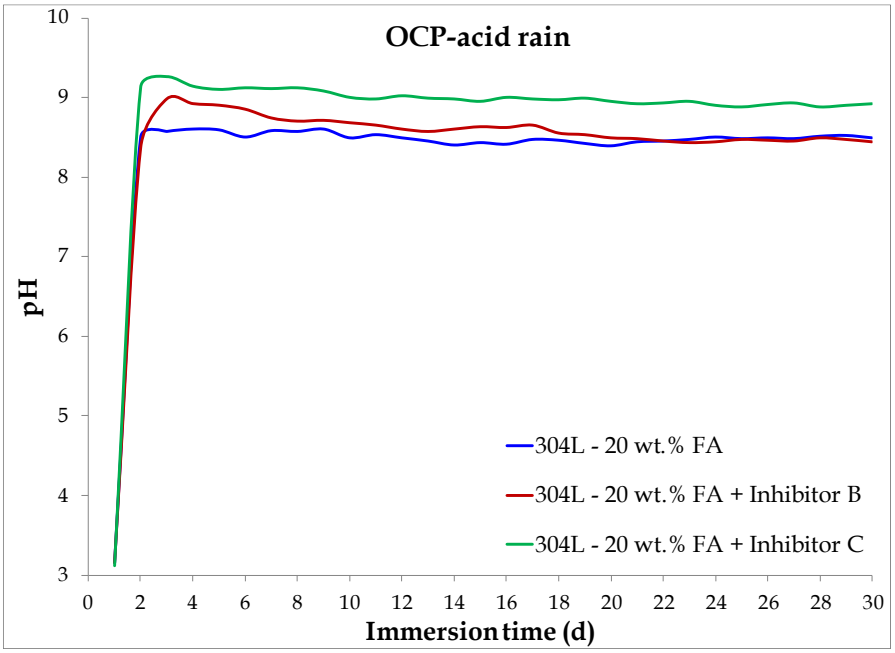


**Fig. 6.** Variation of pH in the acid rain-simulating electrolyte during OCP testing of concrete cubes containing 20 wt.% fly ash with or without the addition of Inhibitors B and C

### 3.3 Microstructural inspection of the corroded rebars

Fig. 7 and Fig. 8 illustrate the SEM cross-sectional micrographs of 304L rebars extracted from concrete cubes the after salt spray test and OCP test, respectively. The concrete cubes contained (a) 20 wt.% FA, (b) Inhibitor B, and (c) Inhibitor C. At this low magnification, an objective overview is provided, showing fine surface states without any signs of corrosion beneath the surfaces.

The excellent performance of the 304L reinforcement under both salt fog and acid rain conditions is evident in Figs. 9 and 10, which manifest the formation of compact and dense CaO-rich surface films containing Si, Al and Mg. The participation of FA in the surface film cannot be discerned, as Ca, Si, Al and Mg are also constituent elements of Portland cement and siliceous sand. However, previous publications concerning electrolytes simulating concrete pore solutions that contained FA and were exposed to saline and acid rain environments, have proven the participation of FA in the surface film and its interaction with the active ions of the electrolytes [7, 24-30]. Furthermore, it is highly likely that the detection of Mg in the surface films shown in Figs. 9 and 10, is owing to the participation of FA in the surface film, as MgO was not detected in the XRD pattern of the concrete used in this study [27].

The participation of Inhibitors B and C in the surface films also cannot be confirmed. However, a hint of nitrogen enrichment on the steel surface can be discerned in Fig. 10a. It should also be noted that nitrogen was automatically detected by the EDX detector. The above observations are in compatibility with Dong et al. [44], who suggested

that inhibitors containing amino groups are more likely to be adsorbed on passive films rather than bare metals, through oxygen vacancies within the passive films that attract the electronegative lone-pair electrons of the nitrogen atom.

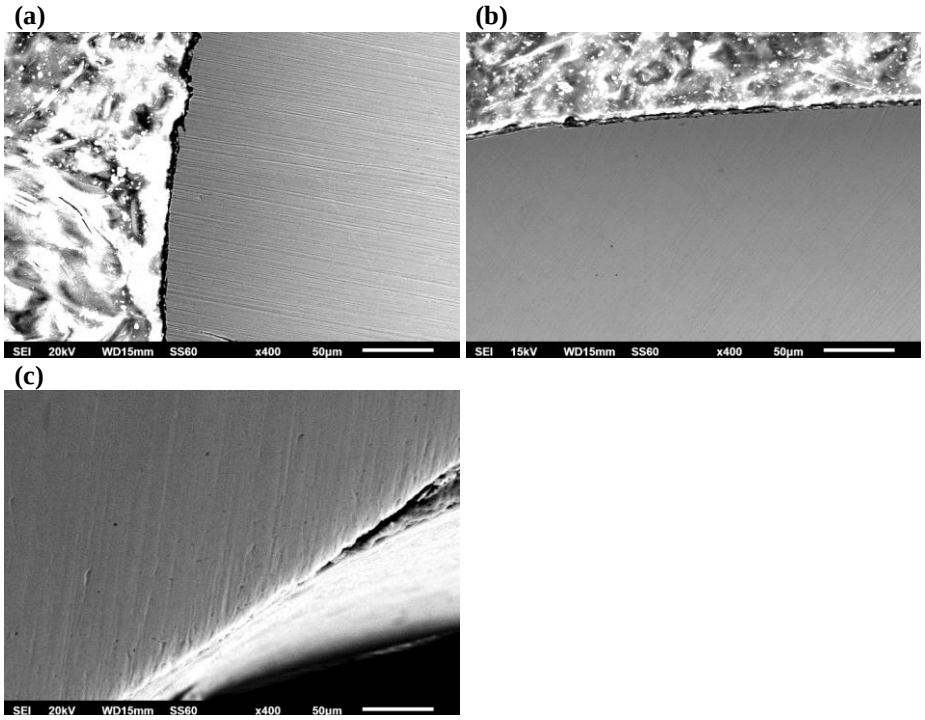


**Fig. 7.** SEM images (cross-sections) of 304L rebars removed from concrete cubes containing (a) 20 wt.% FA, (b) Inhibitor B, (c) Inhibitor C, after salt spraying for 4 m

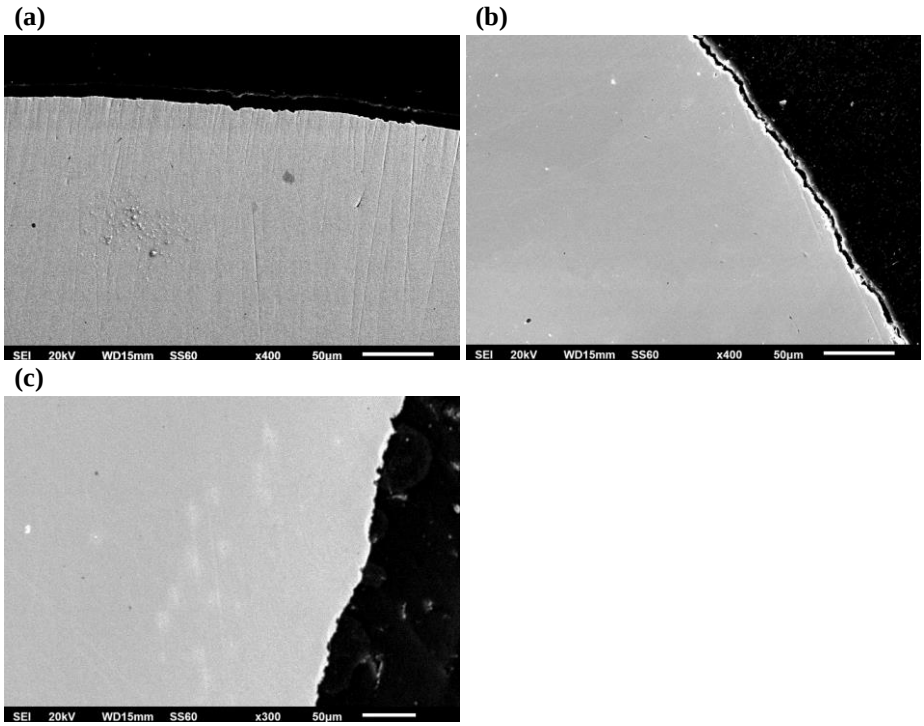


**Fig. 8.** SEM images (cross-sections) of 304L rebars removed from concrete cubes containing (a) 20 wt.% FA, (b) Inhibitor B, (c) Inhibitor C, after OCP testing for 1 m.

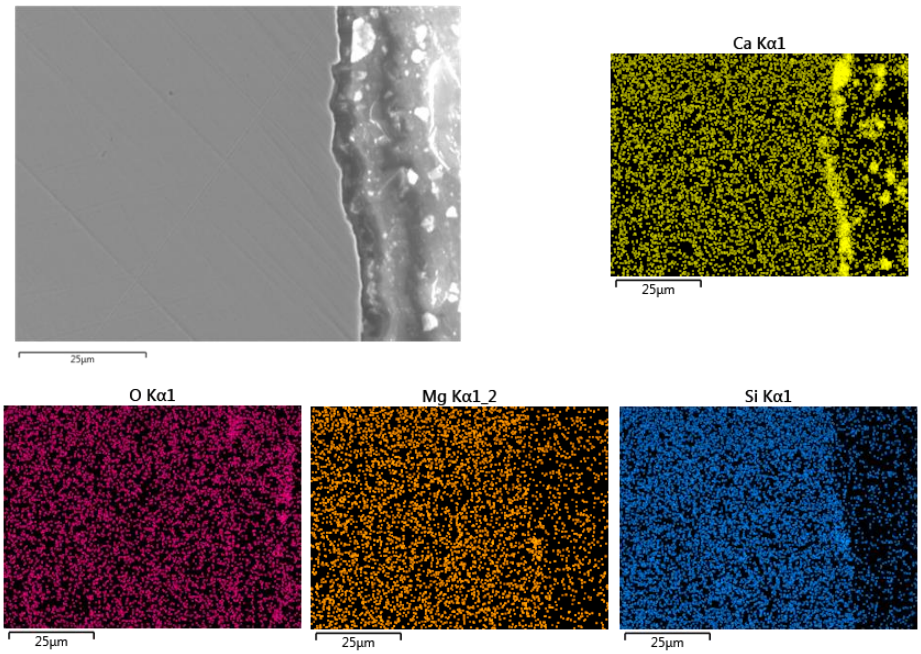


**Fig. 9.** SEM images (cross-sections) of 304L rebar after salt spraying for 4 m (20 wt.% FA + Inhibitor B) and EDX elemental maps.

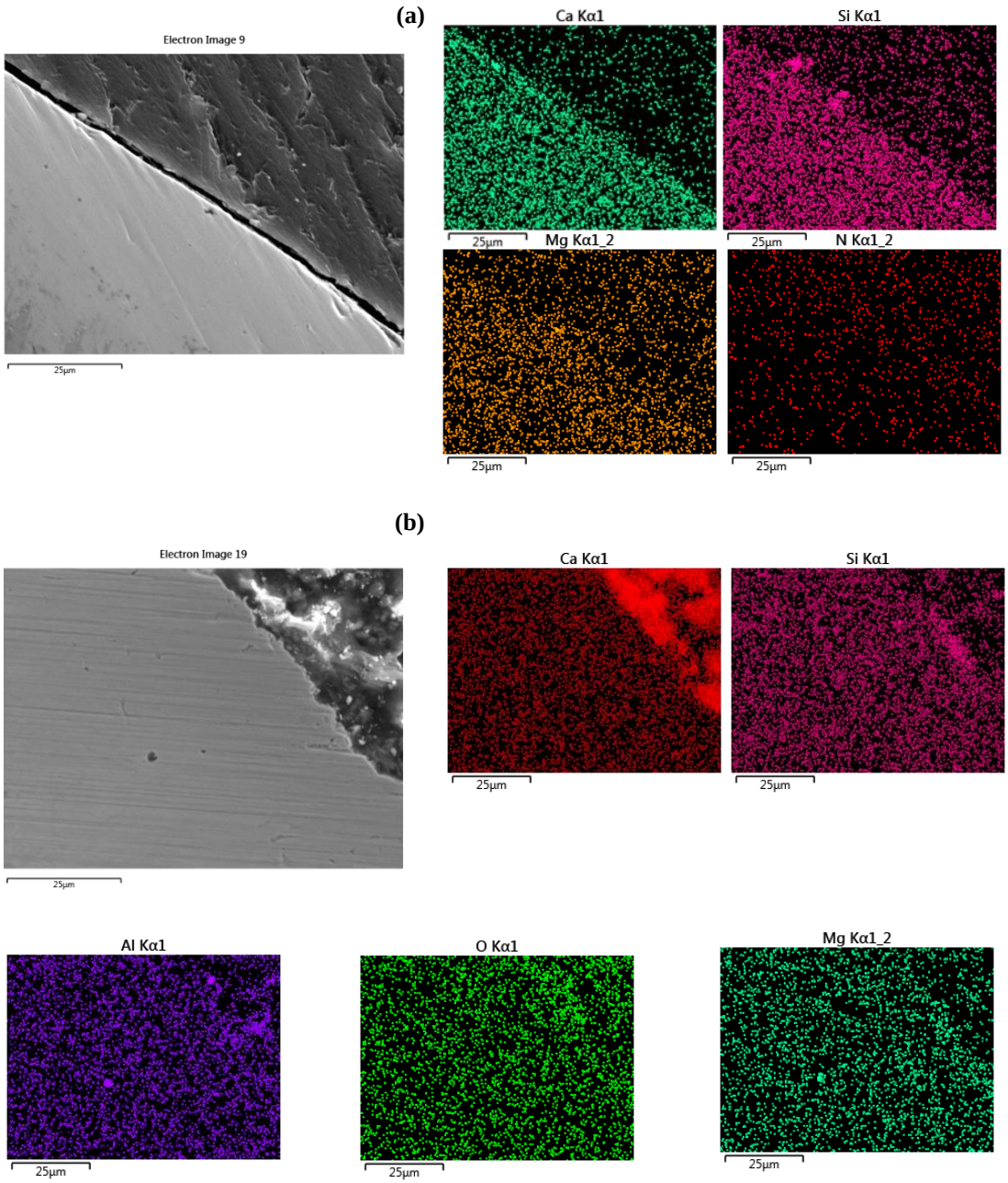


**Fig. 10.** SEM images (cross-sections) of 304L rebars after OCP testing for 1 m. (a) 20 wt.% FA + Inhibitor B, (b) 20 wt.% FA + Inhibitor C, and corresponding EDX elemental maps.

## 4 Conclusions

1. For 304L stainless steel corrugated rebars embedded in concrete cubes containing fly ash (FA), Inhibitor B, Inhibitor C, as well as combinations of FA with Inhibitor B, and immersed in an acid rain (AR) simulating solution for 30 d during an Open Circuit Potential (OCP) test, there is more than a 90% probability that corrosion did not occur.
2. Both Inhibitors B and C improved the corrosion performance of 304L reinforced concrete cubes in AR in the absence of FA. However, when combined with FA, both inhibitors negated the inhibiting effect of FA and vice versa.
3. The 20 wt.% FA content had a beneficial effect on the corrosion behavior of 304L rebars compared to 0 wt.% FA.
4. After an OCP test for 30 d in an AR-simulating electrolyte and after a salt spray test for 4 m (5 wt.% NaCl, 35°C), the presence of 20 wt.% FA combined or not with Inhibitor B did not have any statistically significant effect on the tensile properties of 304L rebars.
5. After 4 m of salt spraying, the 304L reinforcement showed a slight decrease in the strength values, both in the absence and presence of any inhibitors, though within standard deviation. Small decreases in the percent elongation (with or without inhibitors) were also observed. The decreases in percent elongation were statistically significant in all cases except for 20 wt.% FA.
6. After 1 m of OCP testing in the AR simulating electrolyte, the strength values of 304L rebars in the absence of inhibitors and FA, showed small decreases, though within standard deviation. The tensile properties of 304L rebars, in the presence of 20 wt.% FA or Inhibitor B, showed a statistically insignificant but consistent increase. In the case of combined 20 wt.% FA + Inhibitor B, the strength values remained practically unchanged. In all cases except for the absence of any Inhibitors, % elongation increased.
7. Macroscopic examination revealed that the concrete cubes reinforced with 304L rebars, with or without the addition of fly ash and Inhibitors B and C, remained free of corrosion indications after the salt spray and OCP tests. Similarly, cross-sections of the 304L reinforcements did not present any signs of corrosion.
8. Longer OCP testing of reinforced concrete in AR-simulating electrolyte is needed to fully explore the potential of Inhibitor C.

## References

1. Wang, X., Nguyen, M., Stewart, M.G., Syme, M., Leitch, A.: Analysis of Climate Change Impacts on the Deterioration of Concrete Infrastructure. Part 1: Mechanisms, Practices, Modelling and Simulations - A Review. CSIRO, Canberra, Australia (2010).
2. Yalciner, H., Marar, K.: Experimental study on the bond strength of different geometries of corroded and uncorroded reinforcement bars. Journal of Materials in Civil Engineering 29(7), 05017002-1–05017002-10 (2017) https://doi.org/10.1061/(ASCE)MT.1943-5533.0001914.

3. Maia, L., Alves, S.: Low durability of concrete elements due to steel corrosion - cases wherein the steel reinforcing bars acted as an internal clock bomb. Procedia Structural Integrity 5, 139–146 (2017) https://doi.org/10.1016/j.prostr.2017.07.082.
4. Li, Z., Jin, Z., Zhao, T., Wang, P., Zhao, L., Xiong C., Kang, Y.: Service life prediction of reinforced concrete in a sea-crossing railway bridge in Jiaozhou bay: A case study. Applied Sciences 9(7), 1–18 (2019) https://doi.org/10.3390/app9173570.
5. Kepler, J.L., Darwin, D., Locke C.E., Jr.: Evaluation of corrosion protection methods for reinforced concrete highway structures. Structural Engineering and Engineering Materials SM Report No. 58, University of Kansas Center for Research, Inc. Lawrence, Kansas (2000) https://hdl.handle.net/1808/20463.
6. Head, M., Ashby-Bey, E., Edmonds, K., Efe, S., Grose, S., Mason, I.: Stainless steel prestressing strands and bars for use in prestressed concrete girders and slabs. MD-13-SP309B4G Report, Morgan State University, Department of Civil Engineering and Maryland State Highway Administration, Office of Policy & Research (2015).
7. Tsouli, S., Lekatou, A.G. Kleftakis, S.: The effect of fly ash on the corrosion performance of AISI 316L stainless steel reinforced concrete for application to restoration works of ancient monuments. In: Koui, M., Zezza, F., Kouis, D. (eds.) 10th International Symposium on the Conservation of Monuments in the Mediterranean Basin (MONUBASIN),pp. 171–178. Springer, Cham, Switzerland (2018) https://doi.org/10.1007/978-3-319-78093-1_17.
8. Barbhuiya, S., Kumala, D.: Behaviour of a sustainable concrete in acidic environment. Sustainability 9, 1–13 (2017) https://doi.org/10.3390/su9091556.
9. Yu, Z., Ye, G.: The pore structure of cement paste blended with fly ash. Construction and Building Materials 45, 30–35 (2013) https://doi.org/10.1016/j.conbuildmat.2013.04.012.
10. Ghafoori, N., Najimi, M., Diawara, H., Islam, M.S.: Effects of class F fly ash on sulfate resistance of Type V Portland cement concretes under continuous and interrupted sulfate exposures. Construction and Building Materials 78, 85–91 (2015) https://doi.org/10.1016/j.conbuildmat.2015.01.004.
11. Söylev, T.A., Richardson, M.G.: Corrosion inhibitors for steel in concrete: State-of-the-art report. Construction and Building Materials 22(4), 609–622 (2008) https://doi.org/10.1016/j.conbuildmat.2006.10.013.
12. Lee, H.S., Saraswathy, V., Kwon, S.-J., Karthick, S: Corrosion inhibitors for reinforced concrete: A review. In: Aliofkhazraei, M. (ed.), Corrosion inhibitors, principles and recent applications, Chapter 5, IntechOpen, pp. 95–120 (2018) https://doi.org/10.5772/intechopen.72572.
13. Ormellese, M., Bolzoni, F., Goidanich, S., Pedeferri, M.P., Brenna, A.: Corrosion inhibitors in reinforced concrete structures. Part 3 - migration of inhibitors into concrete. Corrosion Engineering, Science and Technology 46(4), 334–339 (2011) https://doi.org/10.1179/174327809X419230.
14. Batis, G., Pantazopoulou, P., Routoulas, A.: Corrosion protection investigation of reinforcement by inorganic coating in the presence of alkanolamine-based inhibitor. Cement and Concrete Composites 25(3), 371–377 (2003) https://doi.org/10.1016/S0958-9465(02)00061-6.
15. Zomorodian, A., Behnood, A.: Review of corrosion inhibitors in reinforced concrete: Conventional and green materials. Buildings 13, 1–20 (2013) https://doi.org/10.3390/buildings13051170.

16. Shi, W., Wang, T.-Z., Dong, Z.-H., & Guo, X.P.: Application of wire beam electrode technique to investigate the migrating behavior of corrosion inhibitors in mortar. Construction and Building Materials 134, 167–175 (2017) https://doi.org/10.1016/j.conbuildmat.2016.12.036.
17. Elsener, B., Angst, U.: Corrosion inhibitors for reinforced concrete, In: Aïtcin, P.C., Flatt, R.J. (eds.), Science and Technology of Concrete Admixtures, Chapter 14, pp. 321–339, Elsevier (2016).
18. Rawat, A., Karade, S.R., Thapliyal, P.C.: Mechanism of inhibitors in control of corrosion of steel in concrete. Materials Today: Proceedings, 1–7 (2023) https://doi.org/10.1016/j.matpr.2023.06.210.
19. Fouda, A.S., Elewady, G.Y., Shalabi, K., Abd El-Aziz, H.K.: Alcamines as corrosion inhibitors for reinforced steel and their effect on cement based materials and mortar performance. RSC Advances 46(5), 36957–36968 (2015) DOI https://doi.org/10.1039/C5RA00717H.
20. Banks L., Hosgood H.: Inhibiting corrosion in reinforced concrete. UK Patent No. WO/1987/006958 (1997).
21. Boyle, B.: A look at developments in vapor phase corrosion inhibitors. Metal Finishing 102(5), 37–41 (2004) https://doi.org/10.1016/S0026-0576(04)90182-1.
22. Bastidas, D.M., Cano, E., Mora, E.M.: Volatile corrosion inhibitors: a review. Anti-Corrosion Methods and Materials 52, 71–77 (2005) https://doi.org/10.1108/00035590510584771.
23. Sherif, El-Sayed M.: The role of corrosion inhibitors in protecting metallic structures against corrosion in harsh environment. In: Fanun, M. (ed.), The role of colloidal systems in environmental protection, Chapter 20, pp. 509–526, Elsevier (2014) https://doi.org/10.1016/B978-0-444-63283-8.00020-X.
24. Tsouli, S., Lekatou, A.G., Kleftakis, S., Matikas, T.E., Dalla, P.T.: Corrosion behavior of 304L stainless steel concrete reinforcement in acid rain using fly ash as corrosion inhibitor. Procedia Structural Integrity 10, 41–48 (2018) https://doi.org/10.1016/j.prostr.2018.09.007.
25. Tsouli, S., Lekatou, A.G., Nikolaidis, C., Kleftakis, S.: Corrosion and tensile behavior of 316L stainless steel concrete reinforcement in harsh environments containing a corrosion inhibitor. Procedia Structural Integrity 17, 268–275 (2019) https://doi.org/10.1016/j.prostr.2019.08.036.
26. Lekatou, A.G., Tsouli, S., Nikolaidis, C., Kleftakis, S., Tragazikis, I.K., Matikas, T.E.: Effect of fly ash on the corrosion performance and structural integrity of stainless steel concrete rebars in acid rain and saline environments. Frattura ed Integrità Strutturale 50, 423–437 (2019) https://doi.org/10.3221/IGF-ESIS.50.36.
27. Lekatou, A.G., Tsouli, S.: Cyclic polarization of corrugated austenitic stainless steel rebars in acid rain: Effect of fly ash, pH and steel type. Corrosion and Materials Degradation 3(1), 75–100 (2022) https://doi.org/10.3390/cmd3010005.
28. Tsouli, S., Lekatou, A.G., Siozos, E., Kleftakis, S.: Accelerated corrosion performance of AISI 316L stainless steel concrete reinforcement used in restoration works of ancient monuments. MATEC Web of Conferences 188(03003), 1–8 (2018) https://doi.org/10.1051/matecconf/201818803003.
29. Tsouli, S., Lekatou, A.G., Goutzos, P., Kleftakis, S.: Effect of fly ash on the electrochemical performance of 316L stainless steel concrete reinforcement in saline environments attacked by acid rain. MATEC Web of Conferences 349(02015), 1–8 (2021) https://doi.org/10.1051/matecconf/202134902015.

30. Tsouli, S., Lekatou, A.G., Kleftakis, S., Gkoutzos, P., Tragazikis, I.K., Matikas, T.E. Combined corrosion inhibitors and mechanical properties of concrete embedded steel (AISI 316L) during accelerated saline corrosion test. Materials Proceedings 5(1), 1–7 (2021) https://doi.org/10.3390/materproc2021005072.
31. Fu, Y., Ding, J., Beaudoin, J.J.: Expansion of Portland cement mortar due to internal sulfate attack. Cement and Concrete Research 27(9), 1299–1306 (1997) https://doi.org/10.1016/S0008-8846(97)00133-6.
32. Martín, D., Seyhan, E.: Protection of reinforced concrete steel exposed to a marine environment - A preliminary onsite study of the performance of a new generation of surface-applied corrosion inhibitors. Corrosion and Materials Degradation 3(4), 628–645 (2022) https://doi.org/10.3390/cmd3040034.
33. Kostakis, G.: Characterization of the fly ashes from the lignite burning power plants of northern Greece based on their quantitative mineralogical composition. Journal of Hazardous Materials 166(2-3), 972–977 (2009) https://doi.org/10.1016/j.jhazmat.2008.12.007.
34. Filippidis, A., Georgakopoulos, A.: Mineralogical and chemical investigation of fly ash from the Main and Northern lignite fields in Ptolemais, Greece. Fuel 71(4), 373–376 (1992).
35. MuCis-mia-200, Technical datasheet, https://sintecno.gr/wp-content/uploads/2023/03/MuCis%C2%AE-mia-200.pdf, last accessed 2024/10/05.
36. QED Margel-580 VPi: Vapour phase Migrating Corrosion Inhibitor in capsule form by Sintecno - Prevention & protection of reinforced concrete structures, https://sintecno.gr/en/diacheomenos-anastoleas-diavrosis-aerias-drasis-se-morfi-kapsoylas-apotin-sintecno-prolipsi-amp-prostasia-kataskeyon-oplismenoy-skyrodematos, last accessed 2024/10/05.
37. Ragab, Kh.A., Abdel-Karim, R., Farag, S., El-Raghy, S.M., Ahmed, H.A.: Influence of SiC, $SiO_2$ and graphite on corrosive wear of bronze composites subjected to acid rain. Tribology International 43(3), 594–601 (2010) https://doi.org/10.1016/j.triboint.2009.09.008.
38. Pérez-Quiroz, J.T., Terán, J., Herrera, M.J., Martínez M., Genescá, J.: Assessment of stainless steel reinforcement for concrete structures rehabilitation. Journal of Constructional Steel Research 64(11), 1317–1324 (2008) https://doi.org/10.1016/j.jcsr.2008.07.024.
39. ASTM International: ASTM C876- 15 Corrosion potentials of uncoated reinforcing steel in concrete, USA (2015).
40. Lee, H., Cho, Y.: Evaluation of the mechanical properties of steel reinforcement embedded in concrete specimen as a function of the degree of reinforcement corrosion. International Journal of Fracture 157(1-2), 81–88 (2009) https://doi.org/10.1007/s10704-009-9334-7
41. Apostolopoulos, Ch.A., Demis, S., Papadakis, V.G.: Chloride-induced corrosion of steel reinforcement - Mechanical performance and pit depth analysis. Construction and Building Materials 38, 139–146 (2013) https://doi.org/10.1016/j.conbuildmat.2012.07.087.
42. Papadakis, V.G.: Effect of fly ash on Portland cement systems: Part II. High-calcium fly ash. Cement and Concrete Research 30(10), 1647–1654 (2000) https://doi.org/10.1016/S0008-8846(00)00388-4.
43. Kerlins, V.: Modes of fracture. In: Schroeder, C.J., Parrington, R.J., Maciejewski, J.O., Lane, J.L. (eds.), ASM Metals Handbook, Volume 12: Fractography, pp. 12-71, ASM International (1987).

44. Dong, Z.H., Shi, W., Zhang, G.A., Guo, X.P.: The role of inhibitors on the repassivation of pitting corrosion of carbon steel in synthetic carbonated concrete pore solution. Electrochimica Acta 56(17), 5890–5897 (2011) https://doi.org/10.1016/j.electacta.2011.04.120.